A20/AN1 zinc-finger proteins positively regulate major latex-like proteins, transporting factors toward dioxin-like compounds in Cucurbita pepo

Fujita, Kentaro ; Yoshihara, Ryouhei ; Hirota, Matashi ; Goto, Junya ; Sonoda, Chihiro ; Inui, Hideyuki

(Citation)
Chemosphere,305:135536

(Issue Date)
2022-10

(Resource Type)
journal article

(Version)
Accepted Manuscript

A20/AN1 zinc-finger proteins positively regulate major latex-like proteins, transporting factors toward dioxin-like compounds in *Cucurbita pepo*

Kentaro Fujita[1] (kentaro.fujita1221@gmail.com) (https://orcid.org/0000-0002-8757-0094)

Ryouhei Yoshihara[2, a] (ryoshihara@mail.saitama-u.ac.jp)

Matashi Hirota[1]

Junya Goto[1]

Chihiro Sonoda[1]

Hideyuki Inui[1, 2, *] (hinui@kobe-u.ac.jp) (https://orcid.org/0000-0002-0981-2641)

[1]Graduate School of Agricultural Science, Kobe University, 1-1 Rokkodaicho, Nada-ku, Kobe, Hyogo 657-8501, Japan

[2]Biosignal Research Center, Kobe University, 1-1 Rokkodaicho, Nada-ku, Kobe, Hyogo 657-8501, Japan

[a]Present address: Graduate School of Science and Engineering, Saitama University, 255 Shimo-Ohkubo, Sakura-ku, Saitama, Saitama 338-8570, Japan.

[*]Corresponding Author:

Hideyuki Inui, Biosignal Research Center, Kobe University,

1-1 Rokkodaicho, Nada-ku, Kobe, Hyogo 657-8501, Japan

E-mail: hinui@kobe-u.ac.jp, Telephone number: +81-78-803-5863

Abstract

The Cucurbitaceae family accumulates dioxin-like compounds in its fruits. We previously showed that *A20/AN1 zinc finger protein* (*ZFP*) genes were highly expressed in the zucchini (*Cucurbita pepo*) subspecies *pepo*, which accumulates dioxin-like compounds at high concentrations. Transgenic tobacco (*Nicotiana tabacum*) plants overexpressing *A20/AN1 ZFP* genes show accumulation of dioxin-like compounds in their upper parts. However, the mechanisms underlying the accumulation of dioxin-like compounds regulated by the A20/AN1 ZFPs remain unclear. Here, we show that A20/AN1 ZFPs positively regulate the expression of the *major latex-like protein* (*MLP*) and its homolog genes in *N. tabacum* and *C. pepo*. MLPs are involved in the transport of dioxin-like compounds from the roots to the upper parts of *C. pepo*. Overexpression of *A20/AN1 ZFP* genes in *N. tabacum* leads to the upregulation of *pathogenesis-related protein class-10* genes with the binding ability toward dioxin-like compounds. Our results demonstrated that A20/AN1 ZFPs upregulate *MLP* and its homolog genes in *N. tabacum* and *C. pepo*, resulting in the accumulation of dioxin-like compounds.

Keywords

A20/AN1 zinc-finger protein; *Cucurbita pepo*; dioxin-like compound; major latex-like protein

Introduction

Dioxin-like compounds are distributed globally and accumulate in humans through bioaccumulation in the food web. The intake of dioxin-like compounds by humans leads to high toxicity such as carcinogenicity and neurotoxicity. It is important to inhibit the uptake of dioxin-like compounds by plants as primary producers in terrestrial ecosystems. However, dioxin-like compounds are detected in agricultural land due to air transportation from e-waste sites of electronic devices (Shen et al., 2009); thus, crop contamination with dioxin-like compounds is a concern. The Cucurbitaceae family, including cucumber (*Cucumis sativus*), melon (*Cucumis melo*), and zucchini (*Cucurbita pepo*), accumulate dioxin-like compounds in their upper parts, unlike other plant families (Otani et al., 2007). *C. pepo*, in particular, accumulates dioxin-like compounds at high concentrations (Hülster et al., 1994; Inui et al., 2011, 2008).

A quantitative difference was found at 17-kDa in the xylem sap proteins of nine *C. pepo* cultivars, and there was a significant positive correlation between the intensity of the 17-kDa protein band and the accumulation level of dioxin-like compounds (Inui et al., 2013). The 17-kDa protein was identified as a major latex-like protein (MLP), a protein of the Bet v 1 family. MLP was first discovered in the latex of the opium poppy (*Papaver somniferum*) (Nessler et al., 1985) and has been identified in several plants (Fujita & Inui 2021). MLPs are involved in the improvement of pathogen resistance (Fujita et al., 2022) and drought tolerance (Wang et al., 2016). The remarkable features of MLPs are their internal hydrophobic cavities and their long transport ability. MLPs bind to steroids (Lytle et al., 2009) and long fatty acids (Choi et al., 2015), and are detected in xylem (Goto et al., 2019) and phloem sap (Gai et al. 2018; Li et al. 2013). These results suggest that MLPs can transport hydrophobic compounds over long distances. MLPs from the Cucurbitaceae family bind dioxin-like compounds *in vitro* and have been detected in the roots and xylem sap (Goto et al. 2019; Inui et al. 2013; Iwabuchi et al. 2020). It is thought that MLPs bind

42 dioxin-like compounds in the roots, and MLP-dioxin-like compound complexes are transported
43 to the aerial parts through xylem vessels. Therefore, MLPs play a crucial role in the accumulation
44 of dioxin-like compounds in the Cucurbitaceae.
45 *C. pepo* shows subspecies differences in the accumulation of dioxin-like compounds; the *C. pepo*
46 ssp. *pepo* accumulates at higher concentrations than that of *C. pepo* ssp. *ovifera* (Inui et al., 2008).
47 *A20/AN1 zinc finger protein* (*ZFP*) genes are highly expressed in the roots of the high accumulator,
48 and there are two types of *A20/AN1 ZFP* genes: the BG type expressed in the high accumulators
49 and the PBG type expressed in the low and high accumulators (Inui et al., 2015). ZFP-BG and
50 ZFP-PBG have A20/AN1 domains, and *A20/AN1 ZFP* genes exist in various eukaryotes such as
51 *Arabidopsis thaliana*, *Dictyostelium discoideum*, *Homo sapiens*, and *Plasmodium falciparum*
52 (Giri et al., 2013). A20/AN1 ZFPs have wide spectra of biological functions, including cell
53 elongation (Liu et al., 2011), drought tolerance (Kang et al., 2017), and pathogen resistance (Liu
54 et al., 2019).
55 Transgenic tobacco plants overexpressing the *aryl hydrocarbon receptor* (*AhR*) have been
56 produced by introducing genes for the DNA-binding domain of bacterial repressor protein LexA,
57 ligand-binding domain of mouse AhR, transcriptional activation domain of virus-derived VP16,
58 and β-glucuronidase (GUS) under the regulation of the 8 × LexA-46 promoter (Kodama et al.,
59 2009). Transgenic tobacco plants take up dioxin-like compounds from their roots, and AhR-
60 dioxin-like compound complexes are formed, which activate the transcription of *GUS*. The
61 accumulation of dioxin-like compounds has been evaluated through the measurement of GUS
62 activity (Inui et al., 2012). Double transgenic tobacco plants overexpressing *AhR* and *A20/AN1*
63 *ZFPs* showed an increase in GUS activity when incubated in a solid medium containing dioxin-
64 like compounds (Inui et al., 2015). This indicates that A20/AN1 ZFPs are involved in the
65 accumulation of dioxin-like compounds (Inui et al., 2015). However, the mechanisms underlying

66 their accumulation through the expression of the *A20/AN1 ZFP* genes remain unclear. Therefore,
67 clarifying the functions of A20/AN1 ZFPs is crucial for understanding the accumulation
68 mechanisms of dioxin-like compounds in *C. pepo*.
69 The purpose of this study is to elucidate of the upregulation mechanisms of *MLP* and its homolog
70 genes by A20/AN1 ZFPs involved in the accumulation of dioxin-like compounds in *C. pepo*.
71 Herein, we show that A20/AN1 ZFPs upregulate *MLP* and its homologous genes by binding to
72 their promoter regions in transgenic tobacco plants and *C. pepo*, thereby promoting the
73 accumulation of dioxin-like compounds. To our knowledge, this is the first study to demonstrate
74 the transcriptional upregulation of *MLP* and its homolog genes by A20/AN1 ZFPs.
75
76 **Materials & Methods**
77 *Construction of a phylogenetic tree*
78 The sequences for the *pathogenesis-related protein class 10* from *Nicotiana tabacum* (*NtPR-10*)
79 genes were obtained from the UniProt database (https://www.uniprot.org/) using the *MLP-PG1*
80 (AB753855) DNA sequence. Phylogenetic reconstructions were performed using "build" of ETE3
81 v3.1.1 (Huerta-Cepas et al., 2016) as implemented in GenomeNet
82 (https://www.genome.jp/tools/ete/). A phylogenetic tree was constructed using FastTree v2.1.8,
83 with the default parameters (Price et al., 2009).
84
85 *Expression analysis*
86 Total RNA was extracted using TRIzol (Thermo Fisher Scientific Inc., Waltham, MA, USA), and
87 cDNA was synthesized from 2.6 μg of total RNA isolated from roots, stems, and leaves of 40-day
88 old *C. pepo* plants by ReverTra Ace qPCR RT Master Mix (Toyobo Co., Ltd., Osaka, Japan)
89 according to the manufacturer's instructions after treatment with DNase I. qRT-PCR (Light Cycler

480 II, Roche Applied Science, Indianapolis, IN, USA) was conducted using the Thunderbird SYBR qPCR Mix (Toyobo) with the primers ZFP-PBG/qPCR-s and ZFP-PBG and BG/qPCR-s for the PBG type, and the ZFP-BG/qPCR-s and ZFP-PBG and BG/qPCR-s for the BG type under the conditions of 1 min at 95°C, 40 cycles of 15 sec at 95°C and 30 sec at 60°C, 5 sec at 95°C, and 1 min at 65°C (Table S1). Subsequently, the samples were heated to 97°C and cooled to 40°C. As an internal standard, the *actin* gene was amplified with CpActin/qPCR-s and CpActin/qPCR-as primers under the same conditions (Table S1) (Inui et al., 2013). The relative expression levels were calculated using the ΔΔCT method.

Total RNA was extracted as described above, and cDNA was synthesized from 0.9 μg of total RNA in the roots of approximately 2-month old sterile-grown tobacco plants using ReverTra Ace qPCR RT Master Mix with gDNA Remover (Toyobo) according to the manufacturer's instructions. qRT-PCR was performed under the above conditions with the primers NtPR-10A/qPCR-s and NtPR-10A/qPCR-as for *NtPR-10A* and NtPR-10B/qPCR-s and NtPR-10B/qPCR-as for *NtPR-10B* (Table S1). These primers recognize some of the *NtPR-10A* and *-10B* genes because of their common sequences within each type. As an internal standard, the tobacco *actin* genes were amplified with the NtActin/qPCR-s and NtActin/qPCR-as primers under the same conditions (Table S1) (Inui et al., 2015). The relative expression levels were calculated using the ΔΔCT method.

Cloning of the NtPR-10A gene from N. tabacum

The leaves of *N. tabacum* 'Samsun NN' that were grown in sterile conditions for approximately 2.5 months in MS medium were used for the extraction of total RNA using TRIzol. cDNA was synthesized using ReverTra Ace qPCR RT Master Mix with gDNA Remover according to the manufacturer's instructions. The gene with the accession number E3W9N3 was cloned as a

114 representative NtPR-10A type with primers E3W9P1-sIF and E3W9P1-asIF using KOD FX Neo
115 (Toyobo) with the annealing temperature at 54°C (Table S1). The sequence was confirmed by
116 DNA sequencing. The fragments were purified using Gel/PCR DNA Isolation System (Viogene-
117 Biotek Corp, Taipei, Taiwan) and inserted into the pET-28b(+) vector (Merck, Darmstadt,
118 Germany) digested with *Nco*I and *Xho*I using the In-Fusion HD Cloning Kit (Takara Bio Inc.,
119 Shiga, Japan), according to the manufacturer's instructions, resulting in pET28-NtPR-10A.
120
121 *Introduction of MLP pro::GUS into transgenic tobacco plants expressing A20/AN1 ZFPs and C.*
122 *pepo and GUS assays.*
123 *MLP-PG1 pro* and *MLP-GR3-2 pro* were cloned as previously described (Fujita et al., 2022,
124 2020a), from *C. pepo* ssp. *ovifera* cv. 'Patty Green' (PG) and ssp. *pepo* cv. 'Magda' (MG),
125 respectively. Promoter regions of *MLP-GR3* genes were cloned using thermal asymmetric
126 interlaced (TAIL) PCR (Liu & Whittier 1995; Liu et al. 1995). First, the 751-bps upstream region
127 of the *MLP-GR3* gene was amplified with random primers and iPCR-MLP-as1 using genomic
128 DNA from cv. PG and cv. MG. Two other specific antisense primers, TAIL-MLP-P-as2 and TAIL-
129 MLP-P-as3, were designed by referring the 751-bps region to amplify further upstream regions
130 (Table S1). PCR was performed with the 2xQuick TaqTM HS DyeMix (Toyobo). Although the
131 reaction conditions for TAIL-PCR followed the PCR conditions shown by Liu et al. (Liu et al.,
132 1995), the annealing temperature of the random hexamer and specific primers were changed to
133 33°C and 53–56°C, respectively. The whole promoter regions of *MLP-GR3* and *MLP-GR3-1* were
134 cloned from the genomes of cv. PG and cv. MG using the primers MG-GR3-1-P-s and MG-GR3-
135 1-P-as as described previously (Fujita et al., 2020a) (Table S1). The sequence was confirmed by
136 DNA sequencing. *MLP-GR3 pro* was inserted into the plant expression vector, pGWB402Ω.

137 The *MLP pro::GUS* constructs were introduced into *R. radiobacter* LBA4404. The overnight
138 culture of the recombinant *R. radiobacter* in Luria-Bertani (LB) medium was suspended in an
139 MMA buffer (10 mM 2-morpholinoethanesulfonic acid [pH5.6], 10 mM $MgCl_2$, 100 μM
140 acetosyringone) to set OD_{600} at 1.0 (Sainsbury and Lomonossoff, 2008). The suspension was
141 incubated at 25°C with continuous shaking for 2 h and injected into the abaxial side of leaves of
142 transgenic tobacco plants that expressed *A20/AN1 ZFPs* and *C. pepo* plants cultivated for
143 approximately two weeks in soil using a needleless syringe. After 6 and 7 days of incubation for
144 the transgenic tobacco plants and *C. pepo*, respectively, 5 mm squares of the injected leaves were
145 sampled and homogenized in protein extraction buffer (50 mM sodium phosphate buffer [pH7.0],
146 10 mM EDTA [pH 8.0], 0.1% [v/v] Triton X-100, 0.1% [w/v] *N*-lauroylsarcosine sodium salt, and
147 0.072% [v/v] 2-mercaptoethanol). After centrifugation at 4°C and 20,700 × *g* for 5 min, the
148 supernatants were collected, and the GUS assay was performed as described in our previous report
149 (Kodama et al., 2009).
150
151 *Purification of the recombinant protein*
152 *NtPR-10A* was expressed in recombinant *Escherichia coli* Rosetta-gami 2 by introducing the
153 plasmid pET28-NtPR-10A, and recombinant NtPR-10A was purified as previously described
154 (Inui et al., 2013). Briefly, recombinant *E. coli* cells were cultured overnight in LB medium
155 containing 100 μg mL^{-1} kanamycin and 50 μg mL^{-1} chloramphenicol at 37°C. After the addition
156 of isopropyl-β-$_D$-thiogalactopyranoside at a final concentration of 0.1 mM, recombinant *E. coli*
157 cells were cultured at 20°C overnight. Cells were washed with 50 mM sodium phosphate buffer
158 ([pH 7.0], 200 mM NaCl) and disrupted by sonication. After centrifugation at 26,700 × *g* for 20
159 min at 4°C, the supernatant was collected and incubated with TALON® metal affinity resin
160 (Takara Bio) for 20 min at 20°C. The mixture was washed with 50 mM sodium phosphate buffer

and loaded onto the column. The 150 mM imidazole in 50 mM sodium phosphate buffer was added, and the elution was collected. SDS-PAGE was performed, and the single band of NtPR-10A at approximately 17 kDa was detected in the elution.

Binding assay

The binding assay was performed as previously described (Inui et al., 2013). Magnetic epoxy beads (Tamagawa Seiki, Co., Ltd, Nagano, Japan) were bound to 25 mM of 4-hydroxy-2′,3,3′,4′,5′-pentachlorobiphenyl (4OH-PeCB106) according to the manufacturer's instructions. The 35 μg mL^{-1} of recombinant NtPR-10A purified from recombinant *E. coli* was incubated with 4OH-PeCB binding beads at 4°C for 4 h in the binding buffer (50 mM potassium phosphate buffer [pH 5.6], 100 mM KCl, 1 mM $MgCl_2$, 0.2 mM $CaCl_2$, 0.2 mM EDTA, 10% [v/v] glycerol, 0.1% [v/v] Nonidet P-40, 1 mM dithiothreitol, 0.2 mM phenylmethylsulfonyl fluoride, 0.1% Triton X-100, and 0.1% *N*-lauroylsarcosine sodium salt). After spinning down and magnetic separation, the supernatant was removed, and the beads were washed eight times with the binding buffer. The binding buffer (35 μL) and 7 μL of a sample buffer solution with a reducing reagent for SDS-PAGE (Nacalai Tesque, Inc., Kyoto, Japan) were added to the beads. The solution was then dispersed and boiled at 98°C for 5 min. After spinning down and magnetic separation, the supernatant was collected as a heat elution sample. The samples were subjected to SDS-PAGE, and the bands were detected using a silver staining kit (Wako Pure Chemical Industries, Ltd., Osaka, Japan).

Construction of the plasmids with ZFP::GFP

The fragments of *ZFP-PBG* and *ZFP-BG* were amplified by PCR with the primers pBI221-PBGs and PBG-GFPas, and pBI221-BGs and PBG-GFPas, respectively (Table S1). For the fusion of

GFP with ZFPs, the *GFP* fragment was amplified with PBG-GFPs and GFP-pBI221as (Table S1). To construct *ZFP-PBG::GFP* and *ZFP-BG::GFP*, a mixture of *GFP* and *ZFP-PBG* or *ZFP-BG* was used as the template for PCR using the primers pBI221-PBGs and GFP-pBI221as, and pBI221-BGs and GFP-pBI221as, respectively (Table S1). *GFP*, as a control, was amplified using the primers pBI221-GFPs and GFP-pBI221as (Table S1). The fusion fragments and *GFP* were inserted into pBI221 digested with *Xba* I and *Sac* I using the In-fusion system.

Subcellular localization

Plasmids carrying *GFP*, *ZFP-PBG::GFP*, or *ZFP-BG::GFP* were introduced into *E. coli*. After incubation in Plusgrowth II medium (Nacalai Tesque) at 37°C overnight, the plasmids were extracted using the Maxi Plus Ultrapure Plasmid Extraction System (Viogene-Biotek Corp) and introduced into the epidermal cells of an onion by particle bombardment using 1.0 μm gold particles and the gene delivery system PDS-1000 (Bio-Rad Laboratories, Inc., Hercules, CA, USA). After overnight incubation in the dark at room temperature, the epidermis was peeled and incubated with 1 μg mL^{-1} 4′,6-diamidino-2-phenylindole dihydrochloride (DAPI) in 50 mM sodium phosphate buffer (pH 7.0) containing 200 mM NaCl for 5–10 min at room temperature. The fluorescence of GFP and DAPI was detected using a fluorescence microscope (ECLIPSE 80i; Nikon Co., Ltd., Tokyo, Japan) through FITC (excitation, 480/30 nm; dichroic mirror, 505 nm; barrier filter, 535/45 nm) and V-2A (excitation, 400/40 nm; dichroic mirror, 430 nm; barrier filter, 440 nm) cubes, respectively, according to previous report (Fukayama et al., 2021).

Statistical analysis

Dunnett's multiple comparison test was used to determine significant differences among treatments using the RStudio software version 1.3.1073 (http://www.rstudio.com).

209

210 **Results**

211 *ZFP genes were expressed in the organs of C. pepo cultivars*

212 Expression analysis of *ZFP* genes was performed with five *C. pepo* ssp. *ovifera* (low accumulator)
213 and four *C. pepo* ssp. *pepo* (high accumulator) cultivars. *ZFP-PBG* was equally expressed, and
214 *ZFP-BG* was also equally expressed in all examined cultivars, except for cv. PG, regardless of the
215 accumulator status (Fig. 1 A and B).

216 The *ZFP::GFP* fusion constructs were introduced into onion epidermal cells by particle
217 bombardment to determine whether A20/AN1 ZFPs were localized in the nucleus and could act
218 as transcription factors. GFP fluorescence was distributed throughout the entire cell following the
219 introduction of the *GFP* construct (Fig. 1 C). In contrast, GFP fluorescence was mainly observed
220 in the nucleus after the introduction of *ZFP-PBG::GFP* and *ZFP-BG::GFP* (Fig. 1 C).

221

222 *NtPR-10A upregulated by ZFP genes bound to a dioxin-like compound*

223 The *NtPR-10* gene sequences were obtained from the UniProt database by applying the *MLP-*
224 *PG1* DNA sequence, and 16 *NtPR-10* genes (*E3W9N3*, *E3W9N4*, *E3W9N5*, *E3W9N6*, *E3W9N7*,
225 *E3W9N8*, *E3W9N9*, *E3W9P0*, *E3W9P1*, *E3W9P2*, *E3W9P3*, *E3W9P6*, *E3W9P7*, *E3W9P8*,
226 *E3W9Q0*, and *E3W9Q1*) were identified. A phylogenetic tree was constructed, and two types of
227 *NtPR-10* genes were observed, *NtPR-10A* and *NtPR-10B* (Fig. 2 A). E3W9N3 and E3W9P8 were
228 most distant from the clade of NtPR-10B and NtPR-10A, respectively, and thus we concluded
229 that E3W9N3 and E3W9P8 could be the representative ones of NtPR-10A and NtPR-10B,
230 respectively, and these genes were used in subsequent assays.

231 Expression analysis of *NtPR-10* genes was performed in transgenic tobacco plants overexpressing
232 *A20/AN1 ZFP* genes to examine the upregulation of *NtPR-10* genes by A20/AN1 ZFPs as

transcription factors. The expression level of *NtPR-10A* in the roots was upregulated in the transgenic tobacco plants overexpressing *ZFP-PBG* by 3.1- (line #5) and 2.6- (line #39) fold and *ZFP-BG* by 1.2- (line #15) and 6.2- (line #45) fold (Fig. 2 B). Upregulation of *NtPR-10A* was not clearly observed in the stems and leaves of transgenic tobacco plants overexpressing *ZFP-PBG* and *ZFP-BG*, except for leaves overexpressing *ZFP-PBG* (Fig. 2 B). In contrast, upregulation of *NtPR-10B* was not observed in the organs of transgenic tobacco plants overexpressing *ZFP-PBG* and *ZFP-BG* (Fig. 2 C). Therefore, *NtPR-10A* was selected as the gene upregulated by A20/AN1 ZFPs.

The binding of NtPR-10A to a dioxin-like compound *in vitro* was investigated using magnetic beads that bind to 4OH-PeCB106. Before the binding assay, we confirmed that the single band was detected by SDS-PAGE of *E. coli* samples expressing *NtPR-10A* (Figure 2D). The detected band was thought to be derived from NtPR-10A. The band was nearly undetectable in the heat elution samples of NtPR-10A incubated with control magnetic beads but was detected in the samples incubated with magnetic beads binding to 4OH-PeCB106 (Fig. 2 D).

A20/AN1 ZFPs upregulated MLP genes

The introduction of the *empty vector*, *MLP-PG1 pro*::*GUS*, *MLP-GR3 pro*::*GUS*, and *MLP-GR3-1 pro*::*GUS* did not increase GUS activity in transgenic tobacco plants overexpressing the *ZFP* genes (Fig. 3 A). In contrast, the introduction of *MLP-GR3-2 pro*::*GUS* increased GUS activity in transgenic tobacco plants overexpressing *ZFP-BG* by 3.78- (line#9 toward VC line#9), 2.76- (line#9 toward VC line#11), 9.40- (line#44 toward VC line#9), and 6.86- (line#44 toward VC line#11) fold (Fig. 3 A).

MLP pro::GUS constructs were transiently introduced into the *C. pepo* ssp. *ovifera* cultivar PG and *C. pepo* ssp. *pepo* cv. MG to investigate the effects of A20/AN1 ZFP on the promoter activity

257 of the *MLP* genes. *R. radiobacter* carrying *MLP pro::GUS* was injected into the *C. pepo* cv. PG
258 and cv. MG. There were almost no differences in the GUS activity of plants by the injection of
259 MMA buffer and *R. radiobacter* expressing the *empty vector* into the PG and MG cultivars (Fig.
260 3 B). In the PG cultivar inoculated with *R. radiobacter* carrying *MLP-PG1 pro::GUS* and *MLP-*
261 *GR3 pro::GUS*, GUS activity was not increased compared to that inoculated with *R. radiobacter*
262 carrying the *empty vector* (Fig. 3 B). In contrast, in the MG cultivar inoculated with *R. radiobacter*
263 carrying *MLP-GR3-1 pro::GUS* and *MLP-GR3-2 pro::GUS*, GUS activity was significantly
264 increased compared to that of the *empty vector* plants by 2.6- and 2.1-fold, respectively (Fig. 3
265 B).
266
267 **Discussion**
268 In the present study, we found that A20/AN1 ZFPs upregulated *MLP* and its homolog genes with
269 the ability to bind to dioxin-like compounds. *A20/AN1 ZFP* genes are highly expressed in high
270 accumulators of dioxin-like compounds in *C. pepo* (Inui et al., 2015). MLPs bind to dioxin-like
271 compounds in root cells, and their complexes are translocated into xylem vessels and transported
272 to the upper parts (Goto et al. 2019; Inui et al. 2013). Herein, we showed that A20/AN1 ZFPs
273 localized in the nucleus, upregulated *NtPR-10A* encoding the protein binding to a dioxin-like
274 compound in transgenic tobacco plants, and bound to the promoter region of *MLP* genes in *C.*
275 *pepo in vivo*. Therefore, our results demonstrated the involvement of A20/AN1 ZFPs in the
276 accumulation of dioxin-like compounds in *C. pepo* through the upregulation of *MLP* genes.
277 To our knowledge, this is the first study to show the upregulation of *MLP* and its homolog genes
278 by A20/AN1 ZFPs. *A20/AN1 ZFP* genes are regulated by abiotic and biotic stresses such as
279 drought (Kang et al., 2017), salinity (Zhao et al., 2021), pathogens (Liu et al., 2019), and plant
280 hormones (Zhang et al., 2016). A20/AN1 ZFPs significantly upregulated abscisic acid (ABA)-,

281 jasmonic acid-, and salicylic acid-responsive genes (Kang et al., 2017; Liu et al., 2019). Recent
282 studies have shown that MLP homologs also respond to abiotic and biotic stresses (Fujita et al.,
283 2022; Fujita and Inui, 2021). MLP43 improves drought tolerance by interacting with sucrose
284 nonfermenting-1-related protein kinase 2 and ABA-responsive element binding factor 1 in the
285 ABA signaling pathway (Wang et al., 2016). MLPs interact with ethylene response factors and
286 promote resistance through the upregulation of *PR* genes (Gai et al. 2018; Yang et al. 2015).
287 Therefore, it appears that A20/AN1 ZFPs confer drought tolerance and resistance against
288 pathogens through the upregulation of *MLP* genes. Furthermore, recent studies have shown that
289 MLPs are localized in xylem and phloem vessels, suggesting that MLPs are transported over long
290 distances between organs (Carella et al. 2016; Gai et al. 2018; Goto et al. 2019; Li et al. 2013). It
291 is possible that A20/AN1 ZFP upregulates *MLP* genes and induces stress responses in distant
292 organs through the transport of MLPs.
293 PR-10s show binding affinity towards plant secondary metabolites and hormones. LI-PR10-2.B
294 from yellow lupine (*Lupinus luteus*) binds to natural and synthetic cytokinin compounds
295 (Fernandes et al., 2009). The binding of PR-10s to dioxin-like compounds has not been
296 investigated. In this study, NtPR-10A showed binding affinity toward 4OH-PeCB106 (Fig. 2 D).
297 Since the cavity of PR-10s is highly hydrophobic and large (Pasternak et al., 2005), NtPR-10A
298 can bind to dioxin-like compounds. Consequently, transgenic tobacco plants overexpressing *ZFP-*
299 *BG* are thought to accumulate high concentrations of dioxin-like compounds (Inui et al., 2015).
300 Hydrophobic organic pollutants in the soil, including dioxin-like compounds, are absorbed by the
301 roots, diffused in the root cells via plasmodesmata, and localized in the endodermis and pericycle
302 (Yamazaki et al., 2015). In *A. thaliana*, tetrachlorodibenzo-*p*-dioxins and polychlorinated
303 biphenyls are taken up from the roots, and the gene expression and the amount of fatty acids are
304 changed (Hanano et al., 2014, 2015, 2018). *MLP* genes are expressed in roots, and MLP-dioxin-

like compound complexes are formed and translocated into xylem vessels (Goto et al., 2019). In this process, A20/AN1 ZFPs play a crucial role in the upregulation of *MLP* genes, probably in the endodermis and pericycle, resulting in the promotion of MLP-dioxin-like compound complex formation (Fig. 4).

The roots of *C. pepo* ssp. *pepo* showed a higher expression level of *MLP-GR3* than those of *C. pepo* ssp. *ovifera*, whereas the latter showed a higher expression level of *MLP-PG1* than that of *C. pepo* ssp. *pepo* (Inui et al., 2013). The roots of *C. pepo* ssp. *ovifera* and *pepo* showed similar expression levels of *ZFP-PBG*, whereas those of *C. pepo* ssp. *pepo* had a higher expression level of *ZFP-BG* than the roots of *C. pepo* ssp. *ovifera* PG (Fig. 1 A and B). Taken together, these results indicate that a high expression level of *ZFP-BG* leads to a high expression level of *MLP-GR3*, and this pattern is consistent with the upregulation of the promoter activity of *MLP-GR3-2* in transgenic tobacco plants overexpressing *ZFP-BG* (Fig. 3 A). As a result, *C. pepo* ssp. *ovifera* and *pepo* accumulate dioxin-like compounds in the aerial parts at low and high concentrations, respectively.

In conclusion, we have revealed the mechanisms underlying the accumulation of dioxin-like compounds in the Cucurbitaceae family. Given that A20/AN1 ZFPs are regulated by abiotic and biotic stresses (Giri et al., 2013), and MLPs confer stress tolerance (Fujita and Inui, 2021), this suggests that A20/AN1 ZFPs originally upregulate *MLP* genes to improve the stress response. MLPs identified in several plants show resistance against pathogens (Fujita et al. 2022; Gai et al. 2018; Yang et al. 2015), suggesting that A20/AN1 ZFPs, particularly ZFP-BG, play a crucial role in pathogen resistance. Furthermore, because MLPs and their homologs, such as PR-10s, have an internal hydrophobic cavity that enables them to bind to dioxin-like compounds, the upregulation of *MLP* and its homolog genes by the expression of *A20/AN1 ZFP* genes leads to phytoremediation by promoting the accumulation of dioxin-like compounds (Inui et al., 2015).

Our previous studies showed that the agrochemical treatment promoted the uptake of hydrophobic organic pollutants in *C. pepo* (Fujita et al., 2020a, 2020b), and thus the upregulation of *A20/AN1 ZFP* genes by the agrochemical treatment also leads to the phytoremediation of dioxin-like compounds.

Author contributions

Kentaro Fujita: Investigation, Methodology, Writing - original draft, Writing - review & editing. **Ryouhei Yoshihara**: Investigation, Methodology, Writing - review & editing. **Matashi Hirota**: Investigation, Methodology, Writing - review & editing. **Junya Goto**: Investigation, Methodology, Writing - review & editing. **Chihiro Sonoda**: Investigation, Methodology, Writing - review & editing. **Hideyuki Inui**: Conceptualization, Funding acquisition, Supervision, Writing - original draft, Writing - review & editing.

Acknowledgments

We thank Dr. Tsuyoshi Nakagawa of Shimane University for providing the plant expression plasmid pGWB402Ω. We sincerely thank Dr. Shigeo Takumi (Graduate School of Agricultural Science, Kobe University), Dr. Kentaro Yoshida (Graduate School of Agricultural Science, Kobe University), and Dr. Hiroshi Fukayama (Graduate School of Agricultural Science, Kobe University) for their advice and assistance.

Funding

This work was supported by Grants-in-Aid for Scientific Research As from the Ministry of Education, Culture, Sports, Science, and Technology of Japan (Nos. 17208029 and 23241028).

Data Availability

The data underlying this article will be shared upon reasonable request to the corresponding author.

Declaration of competing interest

The authors declare that they have no known competing financial interests or personal relationships that could have appeared to influence the work reported in this paper.

References

Carella, P., Merl-Pham, J., Wilson, D.C., Dey, S., Hauck, S.M., Vlot, C., Cameron, R.K., 2016. Comparative Proteomics Analysis of Phloem Exudates Collected During the Induction of Systemic Acquired Resistance. Plant Physiol. 171, 1495–1510. https://doi.org/10.1104/pp.16.00269

Choi, S.H., Hong, M.K., Kim, H.J., Ryoo, N., Rhim, H., Nah, S.Y., Kang, L.W., 2015. Structure of ginseng major latex-like protein 151 and its proposed lysophosphatidic acid-binding mechanism. Acta Crystallogr. Sect. D Biol. Crystallogr. 71, 1039–1050. https://doi.org/10.1107/S139900471500259X

Fernandes, H., Bujacz, A., Bujacz, G., Jelen, F., Jasinski, M., Kachlicki, P., Otlewski, J., Sikorski, M.M., Jaskolski, M., 2009. Cytokinin-induced structural adaptability of a *Lupinus luteus* PR-10 protein. FEBS J. 276, 1596–1609. https://doi.org/10.1111/j.1742-4658.2009.06892.x

Fujita, K., Asuke, S., Isono, E., Yoshihara, R., Uno, Y., Inui, H., 2022. MLP-PG1, a major latex-like protein identified in *Cucurbita pepo*, confers resistance through the induction of pathogenesis-related genes. Planta 255, 10. https://doi.org/10.1007/s00425-021-03795-x

376 Fujita, K., Haga, Y., Yoshihara, R., Matsumura, C., Inui, H., 2020a. Suppression of the
377 expression of genes responsible for transporting of hydrophobic pollutants leads to the
378 production of safer crops. Sci. Total Environ. 741, 140439.
379 https://doi.org/10.1016/j.scitotenv.2020.140439
380 Fujita, K., Inui, H., 2021. Review: Biological functions of major latex-like proteins in plants.
381 Plant Sci. 306, 110856. https://doi.org/10.1016/j.plantsci.2021.110856
382 Fujita, K., Kondoh, Y., Honda, K., Haga, Y., Osada, H., Matsumura, C., Inui, H., 2020b.
383 Pesticide treatment reduces hydrophobic pollutant contamination in *Cucurbita pepo*
384 through competitive binding to major latex-like proteins. Environ. Pollut. 266, 115179.
385 https://doi.org/10.1016/j.envpol.2020.115179
386 Fukayama, H., Miyagawa, F., Shibatani, N., Koudou, A., Sasayama, D., Hatanaka, T., Azuma,
387 T., Yamauchi, Y., Matsuoka, D., Morita, R., 2021. CO2-responsive CCT protein interacts
388 with 14-3-3 proteins and controls the expression of starch synthesis–related genes. Plant
389 Cell Environ. 44, 2480–2493. https://doi.org/10.1111/pce.14084
390 Gai, Y.P., Yuan, S.S., Liu, Z.Y., Zhao, H.N., Liu, Q., Qin, R.L., Fang, L.J., Ji, X.L., 2018.
391 Integrated phloem sap mRNA and protein expression analysis reveals phytoplasma-
392 infection responses in mulberry. Mol. Cell. Proteomics 17, 1702–1719.
393 https://doi.org/10.1074/mcp.RA118.000670
394 Giri, J., Dansana, P.K., Kothari, K.S., Sharma, G., Vij, S., Tyagi, A.K., 2013. SAPs as novel
395 regulators of abiotic stress response in plants. BioEssays 35, 639–648.
396 https://doi.org/10.1002/bies.201200181
397 Goto, J., Iwabuchi, A., Yoshihara, R., Kodama, N., Matsui, T., Hirota, M., Eun, H., Inui, H.,
398 2019. Uptake mechanisms of polychlorinated biphenyls in *Cucurbita pepo* via xylem sap

containing major latex-like proteins. Environ. Exp. Bot. 162, 399–405. https://doi.org/10.1016/j.envexpbot.2019.03.019

Hanano, A., Almousally, I., Shaban, M., 2014. Phytotoxicity effects and biological responses of *Arabidopsis thaliana* to 2,3,7,8-tetrachlorinated dibenzo-*p*-dioxin exposure. Chemosphere 104, 76–84. https://doi.org/10.1016/j.chemosphere.2013.10.060

Hanano, A., Almousally, I., Shaban, M., Moursel, N., Shahadeh, A.A., Alhajji, E., 2015. Differential tissue accumulation of 2,3,7,8-Tetrachlorinated dibenzo-*p*-dioxin in *Arabidopsis thaliana* affects plant chronology, lipid metabolism and seed yield. BMC Plant Biol. 15, 1–13. https://doi.org/10.1186/s12870-015-0583-5

Hanano, A., Shaban, M., Almousally, I., Murphy, D.J., 2018. Identification of a dioxin-responsive oxylipin signature in roots of date palm: involvement of a 9-hydroperoxide fatty acid reductase, caleosin/peroxygenase PdPXG2. Sci. Rep. 8, 1–19. https://doi.org/10.1038/s41598-018-31342-4

Huerta-Cepas, J., Serra, F., Bork, P., 2016. ETE 3: Reconstruction, Analysis, and Visualization of Phylogenomic Data. Mol. Biol. Evol. 33, 1635–1638. https://doi.org/10.1093/molbev/msw046

Hülster, A., Müller, J.F., Marschner, H., 1994. Soil–Plant Transfer of Polychlorinated Dibenzo-p-dioxins and Dibenzofurans to Vegetables of the Cucumber Family (*Cucurbitaceae*). Environ. Sci. Technol. 28, 1110–1115. https://doi.org/10.1021/es00055a021

Inui, H., Gion, K., Utani, Y., Wakai, T., Kodama, S., Eun, H., Kim, Y.S., Ohkawa, H., 2012. Assays of dioxins and dioxin-like compounds in actually contaminated soils using transgenic tobacco plants carrying a recombinant mouse aryl hydrocarbon receptor-mediated β-glucuronidase reporter gene expression system. J. Environ. Sci. Heal. - Part B

Pestic. Food Contam. Agric. Wastes 47, 59–65. https://doi.org/10.1080/03601234.2012.611018

Inui, H., Hirota, M., Goto, J., Yoshihara, R., Kodama, N., Matsui, T., Yamazaki, K., Eun, H., 2015. Zinc finger protein genes from *Cucurbita pepo* are promising tools for conferring non-Cucurbitaceae plants with ability to accumulate persistent organic pollutants. Chemosphere 123, 48–54. https://doi.org/10.1016/j.chemosphere.2014.11.068

Inui, H., Sawada, M., Goto, J., Yamazaki, K., Kodama, N., Tsuruta, H., Eun, H., 2013. A Major Latex-Like Protein Is a Key Factor in Crop Contamination by Persistent Organic Pollutants. Plant Physiol. 161, 2128–2135. https://doi.org/10.1104/pp.112.213645

Inui, H., Wakai, T., Gion, K., Kim, Y.S., Eun, H., 2008. Differential uptake for dioxin-like compounds by zucchini subspecies. Chemosphere 73, 1602–1607. https://doi.org/10.1016/j.chemosphere.2008.08.013

Inui, H., Wakai, T., Gion, K., Yamazaki, K., Kim, Y.-S., Eun, H., 2011. Congener Specificity in the Accumulation of Dioxins and Dioxin-Like Compounds in Zucchini Plants Grown Hydroponically. Biosci. Biotechnol. Biochem. 75, 705–710. https://doi.org/10.1271/bbb.100833

Iwabuchi, A., Katte, N., Suwa, M., Goto, J., Inui, H., 2020. Factors regulating the differential uptake of persistent organic pollutants in cucurbits and non-cucurbits. J. Plant Physiol. 245, 153094. https://doi.org/10.1016/j.jplph.2019.153094

Kang, M., Lee, S., Abdelmageed, H., Reichert, A., Lee, H.K., Fokar, M., Mysore, K.S., Allen, R.D., 2017. Arabidopsis stress associated protein 9 mediates biotic and abiotic stress responsive ABA signaling via the proteasome pathway. Plant Cell Environ. 40, 702–716. https://doi.org/10.1111/pce.12892

445 Kodama, S., Okada, K., Akimoto, K., Inui, H., Ohkawa, H., 2009. Recombinant aryl
446 hydrocarbon receptors for bioassay of aryl hydrocarbon receptor ligands in transgenic
447 tobacco plants. Plant Biotechnol. J. 7, 119–128. https://doi.org/10.1111/j.1467-
448 7652.2008.00378.x
449 Li, P., Chen, L., Zhou, Y., Xia, X., Shi, K., Chen, Z., Yu, J., 2013. Brassinosteroids-Induced
450 Systemic Stress Tolerance was Associated with Increased Transcripts of Several Defence-
451 Related Genes in the Phloem in *Cucumis sativus*. PLoS One 8, 1–8.
452 https://doi.org/10.1371/journal.pone.0066582
453 Liu, S., Wang, J., Jiang, S., Wang, H., Gao, Y., Zhang, H., Li, D., Song, F., 2019. Tomato
454 SlSAP3, a member of the stress-associated protein family, is a positive regulator of
455 immunity against *Pseudomonas syringae* pv. *tomato* DC3000. Mol. Plant Pathol. 20, 815–
456 830. https://doi.org/10.1111/mpp.12793
457 Liu, Y. -G, Mitsukawa, N., Oosumi, T., Whittier, R.F., 1995. Efficient isolation and mapping of
458 *Arabidopsis thaliana* T-DNA insert junctions by thermal asymmetric interlaced PCR.
459 Plant J. https://doi.org/10.1046/j.1365-313X.1995.08030457.x
460 Liu, Y., Xu, Y., Xiao, J., Ma, Q., Li, D., Xue, Z., Chong, K., 2011. OsDOG, a gibberellin-
461 induced A20/AN1 zinc-finger protein, negatively regulates gibberellin-mediated cell
462 elongation in rice. J. Plant Physiol. 168, 1098–1105.
463 https://doi.org/10.1016/j.jplph.2010.12.013
464 Liu, Y.G., Whittier, R.F., 1995. Thermal asymmetric interlaced PCR: automatable amplification
465 and sequencing of insert end fragments from P1 and YAC clones for chromosome
466 walking. Genomics 25, 674–681. https://doi.org/10.1016/0888-7543(95)80010-J
467 Lytle, B.L., Song, J., de la Cruz, N.B., Peterson, F.C., Johnson, K.A., Bingman, C.A., Phillips,
468 G.N., Volkman, B.F., 2009. Structures of two *Arabidopsis thaliana* major latex proteins

represent novel helix-grip folds. Proteins Struct. Funct. Bioinforma. 76, 237–243. https://doi.org/10.1002/prot.22396

Nessler, C.L., Allen, R.D., Galewsky, S., 1985. Identification and Characterization of Latex-Specific Proteins in Opium Poppy. Plant Physiol. 79, 499–504. https://doi.org/10.1104/pp.79.2.499

Otani, T., Seike, N., Sakata, Y., 2007. Differential uptake of dieldrin and endrin from soil by several plant families and *Cucurbita* genera. Soil Sci. Plant Nutr. 53, 86–94. https://doi.org/10.1111/j.1747-0765.2007.00102.x

Pasternak, O., Biesiadka, J., Dolot, R., Handschuh, L., Bujacz, G., Sikorski, M.M., Jaskolski, M., 2005. Structure of a yellow lupin pathogenesis-related PR-10 protein belonging to a novel subclass. Acta Crystallogr. Sect. D Biol. Crystallogr. 61, 99–107. https://doi.org/10.1107/S0907444904028173

Price, M.N., Dehal, P.S., Arkin, A.P., 2009. Fasttree: Computing large minimum evolution trees with profiles instead of a distance matrix. Mol. Biol. Evol. 26, 1641–1650. https://doi.org/10.1093/molbev/msp077

Sainsbury, F., Lomonossoff, G.P., 2008. Extremely high-level and rapid transient protein production in plants without the use of viral replication. Plant Physiol. 148, 1212–1218. https://doi.org/10.1104/pp.108.126284

Shen, C., Chen, Y., Huang, S., Wang, Z., Yu, C., Qiao, M., Xu, Y., Setty, K., Zhang, J., Zhu, Y., Lin, Q., 2009. Dioxin-like compounds in agricultural soils near e-waste recycling sites from Taizhou area, China: Chemical and bioanalytical characterization. Environ. Int. 35, 50–55. https://doi.org/10.1016/j.envint.2008.07.005

Wang, Y., Yang, L., Chen, X., Ye, T., Zhong, B., Liu, R., Wu, Y., Chan, Z., 2016. *Major latex protein-like protein 43* (*MLP43*) functions as a positive regulator during abscisic acid

responses and confers drought tolerance in *Arabidopsis thaliana*. J. Exp. Bot. 67, 421–434. https://doi.org/10.1093/jxb/erv477

Yamazaki, K., Tsuruta, H., Inui, H., 2015. Different uptake pathways between hydrophilic and hydrophobic compounds in lateral roots of *Cucurbita pepo*. J. Pestic. Sci. 40, 99–105. https://doi.org/10.1584/jpestics.D14-081

Yang, C.L., Liang, S., Wang, H.Y., Han, L.B., Wang, F.X., Cheng, H.Q., Wu, X.M., Qu, Z.L., Wu, J.H., Xia, G.X., 2015. Cotton major latex protein 28 functions as a positive regulator of the ethylene responsive factor 6 in defense against *Verticillium dahliae*. Mol. Plant 8, 399–411. https://doi.org/10.1016/j.molp.2014.11.023

Zhang, Y., Lan, H., Shao, Q., Wang, R., Chen, H., Tang, H., Zhang, H., Huang, J., 2016. An A20/AN1-type zinc finger protein modulates gibberellins and abscisic acid contents and increases sensitivity to abiotic stress in rice (*Oryza sativa*). J. Exp. Bot. 67, 315–326. https://doi.org/10.1093/jxb/erv464

Zhao, X., Wang, R., Zhang, Y., Li, Y., Yue, Y., Zhou, T., Wang, C., 2021. Comprehensive analysis of the stress associated protein (SAP) gene family in *Tamarix hispida* and the function of *ThSAP6* in salt tolerance. Plant Physiol. Biochem. 165, 1–9. https://doi.org/10.1016/j.plaphy.2021.05.016

Supporting information

Additional supporting information may be found online in the Supporting Information section at the end of the article: Table S1. Sequences of the primers; Table S2. information of plasmids and host bacterial strains

Figure legends

517 Figure 1. *A20/AN1 zinc finger protein* (*ZFP*) genes are ubiquitously expressed in the organs of
518 *Cucurbita pepo*.
519 (A) (B) Expression level of *A20/AN1 ZFP* genes in the organs of *C. pepo* cultivars. The cultivars
520 of *C. pepo* were cultivated at 25°C for 40 days. Total RNA was extracted from the roots, stems,
521 and leaves, and qRT-PCR was performed (*n*=3–4). The sequence of the primers is listed in Table
522 S1. The expression level in each organ was calculated relative to that of PG. The same data as
523 Inui et al., 2015 were used in the expression level of PG, BB, and GR. BB, cv. 'Black Beauty';
524 GR, cv. 'Gold Rush'; MG, cv. 'Magda'; PG, cv. 'Patty Green'; RA, cv. 'Raven'; SB, cv.
525 'Sunburst'; SR, cv. 'Sunray'; ST, cv. 'Starship'; ZP, cv. 'Zephyr'.
526 (C) Subcellular localization of A20/AN1 ZFPs. The pBI221 vector containing *GFP*, *ZFP-*
527 *PBG::GFP*, and *ZFP-BG::GFP* were transiently introduced into the epidermal cells of an onion
528 by particle bombardment. After the incubation with 4′,6-diamidino-2-phenylindole
529 dihydrochloride (DAPI), the fluorescence of GFP and DAPI in the epidermal cells was observed.
530
531 Figure 2. Pathogenesis-related protein class 10 from *Nicotiana tabacum* (NtPR-10) binds to
532 dioxin-like compounds.
533 (A) Phylogenetic tree of *NtPR-10* genes. The sequences for *NtPR-10* genes were obtained from
534 the database of UniProt (https://www.uniprot.org/) by application of the *MLP-PG1* DNA
535 sequence. Phylogenetic reconstructions were performed using "build" of ETE3 v3.1.1 (Huerta-
536 Cepas et al., 2016), and the phylogenetic tree was constructed using FastTree v2.1.8 with the
537 default parameters (Price et al., 2009). The selected gene from *NtPR-10A* and *NtPR-10B*,
538 respectively, is shown in red.
539 (B) (C) Upregulation of *NtPR-10* by *A20/AN1 zinc finger protein* (*ZFP*) genes. Transgenic
540 tobacco plants overexpressing *ZFP-BG and ZFP-PBG* were cultivated at 25°C for 2 months. Total

RNA was extracted from the roots, stems, and leaves, and qRT-PCR was performed. The sequence of the primers is listed in Table S1. The expression level in each organ was calculated relative to that of line #9 of the transgenic tobacco plants expressing *empty vector*. VC, transgenic tobacco plants expressing *empty vector*; *35S::ZFP-PBG*, transgenic tobacco plants overexpressing *ZFP-PBG*; *35S::ZFP-BG*, transgenic tobacco plants overexpressing *ZFP-BG*; AhR, aryl hydrocarbon receptor.

(D) Binding of NtPR-10A toward PCB. The 25 mM of 4-hydroxy-2′,3,3′,4′,5′-pentachlorobiphenyl (4OH-PeCB106) binding magnetic beads were prepared. Recombinant NtPR-10A was incubated with 4OH-PeCB106 binding beads at 4°C for 4 h. After washing and heat elution, the samples were subjected to SDS-PAGE, and the bands were detected by silver staining. Recombinant NtPR-10A was subjected to SDS-PAGE as an input sample.

Figure 3. A20/AN1 zinc finger proteins (ZFPs) upregulate *major latex-like protein* (*MLP*) genes. (A) (B) β-Glucuronidase (GUS) activity of the transgenic tobacco plants overexpressing *A20/AN1 ZFP* genes and *Cucurbita pepo* transiently expressing *MLP-pro::GUS*. The transgenic tobacco plants and *C. pepo* subspecies *ovifera* cultivar 'Patty Green' and ssp. *pepo* cv. 'Magda' were cultivated at 25°C for approximately two weeks and inoculated with *Rhizobium radiobacter* carrying *MLP-pro::GUS*. After 6 and 7 days of incubation for the transgenic tobacco plants and *C. pepo*, respectively, GUS activity was measured in the transgenic tobacco plants (A) and *C. pepo* (B). -, buffer; *EV*, *R. radiobacter* carrying *empty vector*; *VC*, transgenic tobacco plants transformed with *empty vector*; *35S::ZFP-PBG*, transgenic tobacco plants overexpressing *ZFP-PBG*; *35S::ZFP-BG*, transgenic tobacco plants overexpressing *ZFP-BG*; AhR, aryl hydrocarbon receptor. Asterisks indicate the significant differences compared to GUS activity in plants injected with the *EV* by Dunnett's multiple comparison test (*, $p < 0.05$).

565

566 Figure 4. A20/AN1 zinc finger proteins (ZFPs) play a crucial role in the accumulation of dioxin-

567 like compounds via upregulation of *major-latex-like protein* (*MLP*) genes in *Cucurbita pepo*.

(A) *ZFP-PBG*

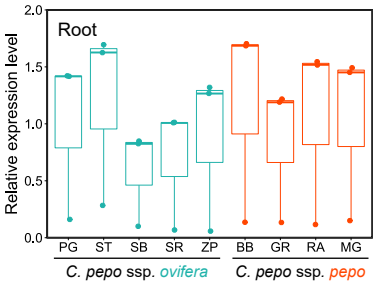

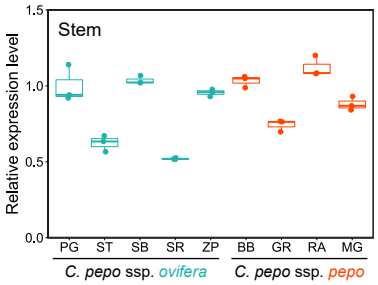

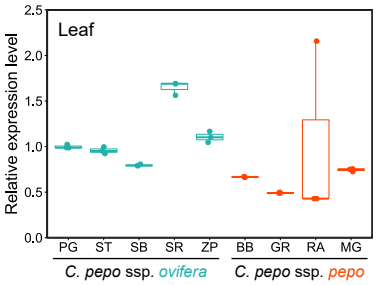

(B) *ZFP-BG*

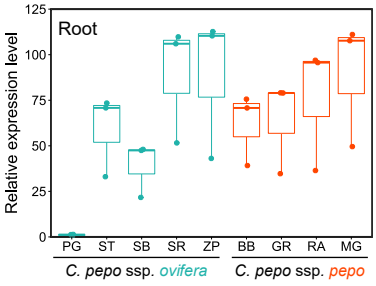

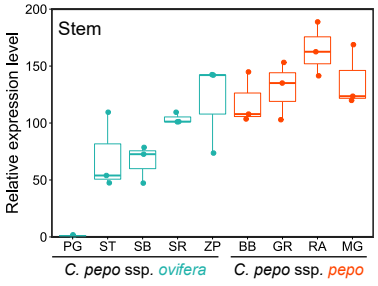

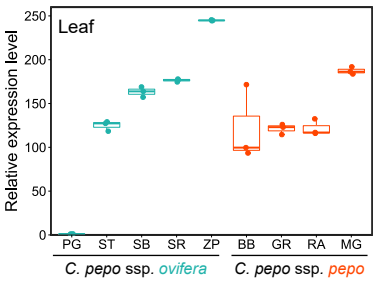

(C)

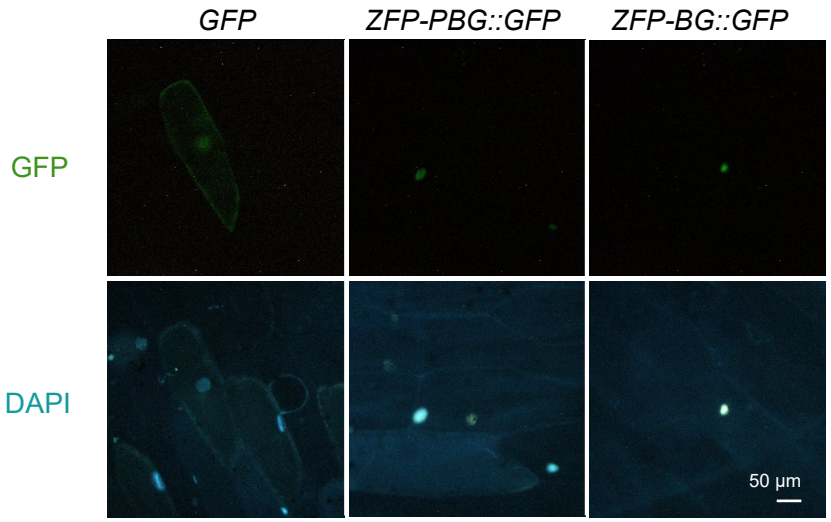

Figure 1

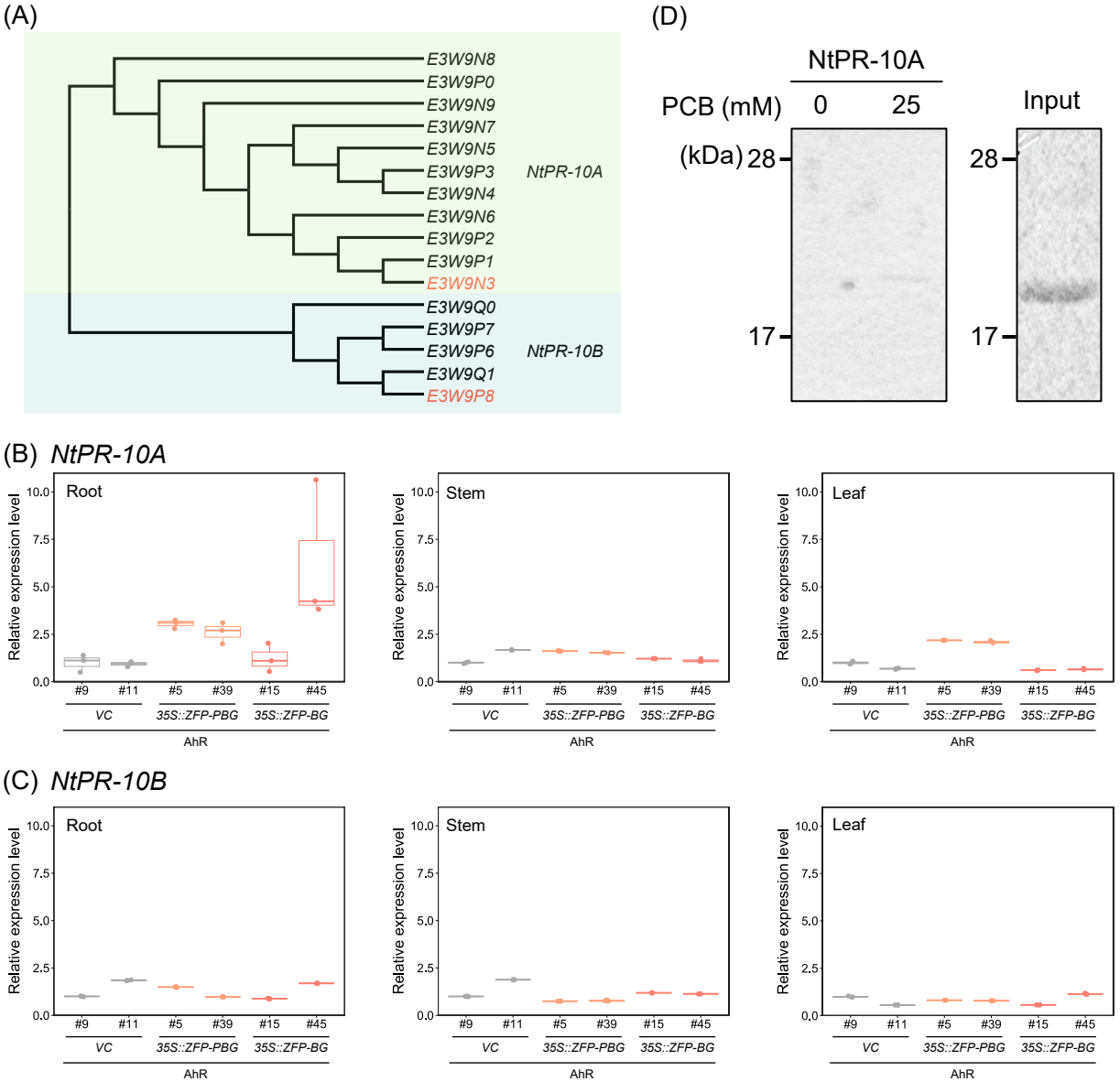
(A)
E3W9N8
E3W9P0
E3W9N9
E3W9N7
E3W9N5
E3W9P3
E3W9N4
E3W9N6
E3W9P2
E3W9P1
E3W9N3
E3W9Q0
E3W9P7
E3W9P6
E3W9Q1
E3W9P8
NtPR-10A
NtPR-10B
(D)
NtPR-10A
PCB (mM)
0
25
Input
(kDa)
28
17
28
17
(B) NtPR-10A
Root
Stem
Leaf
Relative expression level
10.0
7.5
5.0
2.5
0.0
#9
#11
#5
#39
#15
#45
VC
35S::ZFP-PBG
35S::ZFP-BG
AhR
(C) NtPR-10B
Root
Stem
Leaf
Relative expression level
AhR

Figure 2

(A)

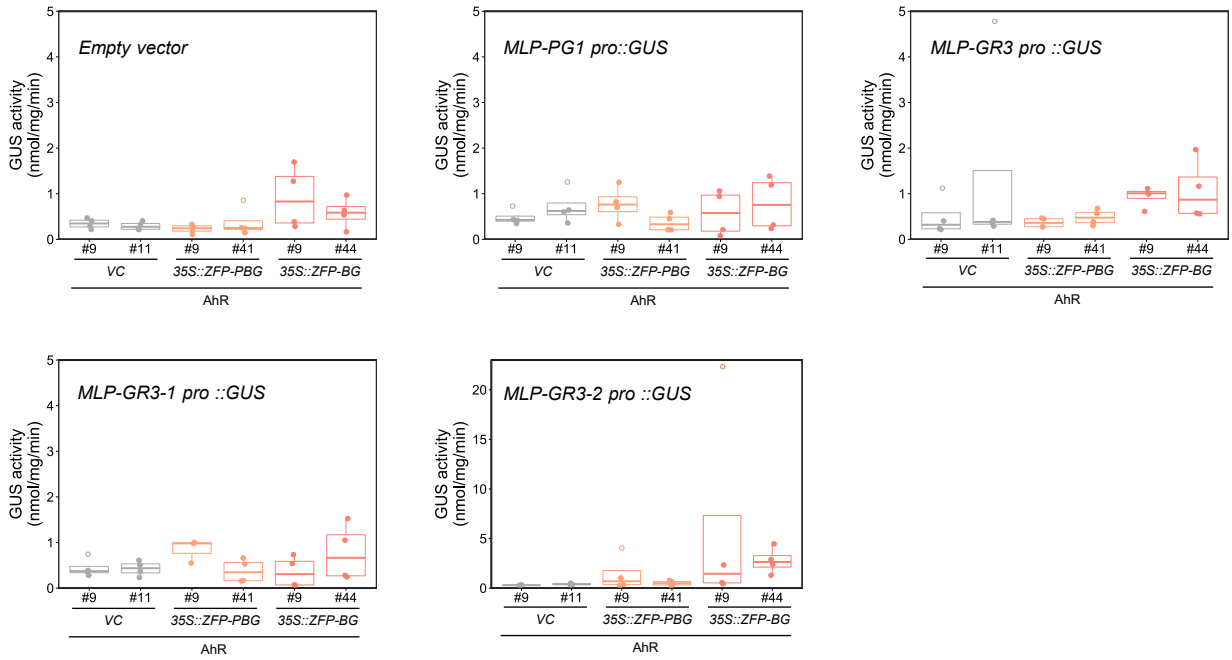
Empty vector
MLP-PG1 pro::GUS
MLP-GR3 pro ::GUS
MLP-GR3-1 pro ::GUS
MLP-GR3-2 pro ::GUS
GUS activity (nmol/mg/min)
#9
#11
#9
#41
#9
#44
VC
35S::ZFP-PBG
35S::ZFP-BG
AhR

(B)

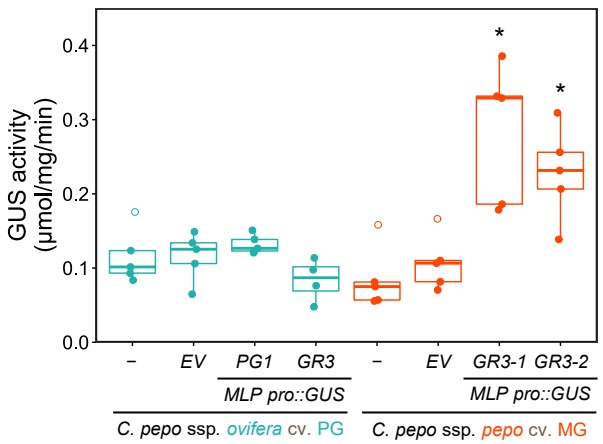
GUS activity (µmol/mg/min)
0.0
0.1
0.2
0.3
0.4
*
*
–
EV
PG1
GR3
–
EV
GR3-1
GR3-2
MLP pro::GUS
MLP pro::GUS
C. pepo ssp. ovifera cv. PG
C. pepo ssp. pepo cv. MG

Figure 3

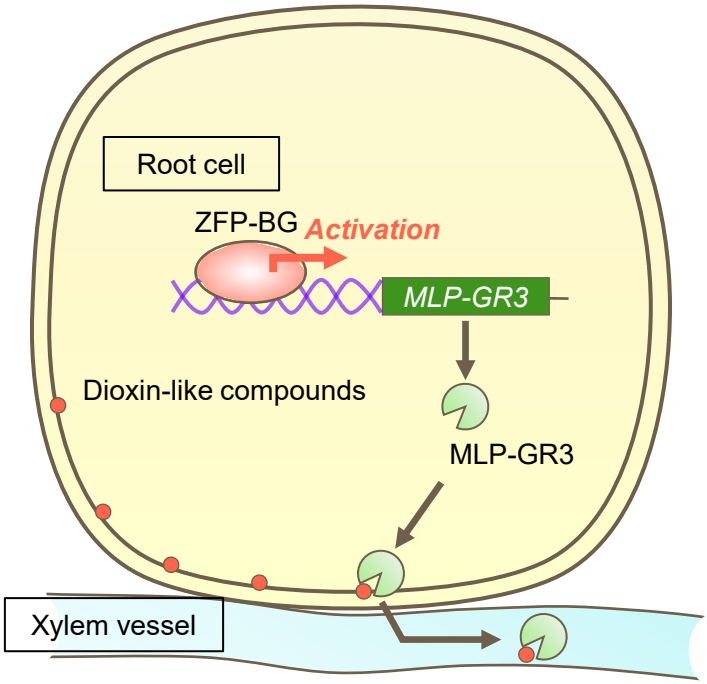
Root cell
ZFP-BG
Activation
MLP-GR3
Dioxin-like compounds
MLP-GR3
Xylem vessel

Figure 4